Published in: Proceedings of the 10th International Geoscience and Remote Sensing Symposium (IGARSS '90), May 20-24, 1990, The University of Maryland, College Park, Maryland

MODEL FOR 3-D OPTICAL IMAGING OF TISSUE

R.L. Barbour, H. Graber, R. Aronson* and J. Lubowsky

Departments of Pathology and Biophysics, SUNY Health Science Center at Brooklyn, Brooklyn, NY, 11203, (718)-270-1661, and *Department of Physics, Polytechnic University, Brooklyn, NY 11201

ABSTRACT

A potential imaging scheme is described which considers use of reflected radiation at near infrared frequencies and is intended for use in a broad spectrum of clinical applications. For clinical studies the object is to detect and locate regions of anomalous absorption which yield information about physiological function. Using Monte Carlo procedures to simulate the process the relations between detector response and the paths of contributing photons were calculated. This information was then processed using a backprojection scheme to compute 3-D images of random media containing discrete absorbers (simulating tissue). The current report demonstrates the feasibility of 3-D imaging of subsurface structures in random media based on the analysis of diffusely scattered light. [Key words; Imaging, Random Media, Optical, Backscatter].

INTRODUCTION

The past several years have seen the development of a variety of techniques for medical imaging, including X-ray computed tomography (CT), magnetic resonance imaging (MRI), ultrasound, and positron emission tomography (PET). While these techniques provide highly useful information about the structure of tissue, with the possible exception of PET they give little to no information about its functional properties. Optical techniques, on the other hand, do hold the potential to yield such information. This is based on the known close association between organ function and oxidative metabolism and, in turn, the oxidation state of heme proteins [1].

Our interest in this problem has been to consider the possibility of reconstructing 3-D optical images which identify local differences in the oxygenation state of tissue. Because light is intensely scattered by tissue, there is no well-defined path for the radiation between source and receiver. In principle an infinite number of paths is possible, and the entire volume of the medium has been illuminated to some degree by the detected light. While a first consideration of this problem might indicate that it is unsolvable, results here show that selective interrogation of the subsurface properties of a random medium can be obtained by examining the relationships between the distribution of paths of emerging light and the position and orientation of the receiver. Results presented also show that by evaluating the detector response in terms of its weight function, a backprojection scheme can be employed to calculate a 3-D image of subsurface absorbers. Portions of this work have been communicated in preliminary form [2,3].

METHODS

As a starting point, photon transport in tissue was modeled by a Monte Carlo method in which photons were directed normally to a medium having infinite length and width and finite thickness. The distance between collisions was an exponentially distributed random variable and scattering was isotropic. The absorption cross-section varied from 0-10% of the total cross-section in the calculations of photon path distributions, but was zero for calculations of collision density and simulations of reflectance measurements of the imaging problem. The unit of length was the photon's mean free path (MFP).

Detector Configuration: In the calculations of photon path distributions, each detector measured the outgoing flux within a 1-MFP-wide annulus centered at the point of injection. Each annulus encompassed twelve detectors, each selective for photons whose direction on emergence fell into a different 90° wide interval of azimuthal angles and 30° wide interval of elevation angles. In the calculations of internal collision densities, each voxel was a detector, and no attempt was made at discriminating the direction of entry or exit by a photon from a voxel. In the reflectance measurement simulations for the imaging problem, each detector measured the outgoing flux within a 1-square-MFP patch on the medium's surface and in directions deviating by up to 10° from the detector's central axis. The solid angle subtended by these detectors was about 0.03π sr.

Efficiency of Simulation: The efficiency of the simulations was maximized by considering the propagation of photon ensembles and by employing the techniques of renormalization and Russian roulette. In the simulations of reflectance measurements for the imaging problem, the efficiency was further increased by biasing the distribution of scattering angles to favor scattering toward the incident surface slightly over scattering away from it. The bias was compensated for by adjusting the photon's weight [4].

CH2825-8/90/0000-01395/$01.00

To reduce the effect of statistical fluctuations, correlated sampling was used where applicable. In the calculations of photon path distributions all values for the absorption cross-section were modeled simultaneously, with the same photon histories in each but a different weight for each medium. In the reflectance measurement simulations a single set of photons was simultaneously propagated through two media, one containing heterogeneous absorbers and the other without them; the two media were identical otherwise. This procedure ensured that the difference between the photon fluxes for the two media, in any given detector, was due only to the presence of heterogeneities.

Scoring: For the calculations of internal collision densities, the quantity scored in each voxel was the sum of the pre-collision weights of all photons that had collision within the 1-cubic-MFP volume of the voxel. The sum of the squares of these weights were also accumulated for calculation of standard errors. The densities were reported in units of collisions/unit volume/incident photon. In the calculations of photon path distributions and simulations of reflectance measurements, a last-collision statistical estimation procedure was used to calculate the flux at the detector [4]. The fluxes and their standard errors were reported in units of photons detected/incident photon/unit area/steradian. In the calculations of photon path distributions, each photon was tracked as it propagated in the medium, and at every collision the greatest depth it had reached to that point, the number of collisions it had undergone, and the total distance it had traveled were stored. These quantities were multiplied by the photon's weight and they and their squares were used to calculate the average maximum depth, **<Z>**, average number of collisions, **<n>**, and average total pathlength, **<d>** of light received by each detector, together with the associated standard errors.

Calculation of Weight Functions: In a random medium all points in space contribute to the detector response to a variable extent. In the limit of weak absorption, the effect local absorption has on this response is given by:

$$\Delta \Phi_i = \int_V \frac{\Sigma_a(\vec{r})}{\Sigma_t(\vec{r})} \Psi(\vec{r}) P(\vec{r}) \, d(\vec{r}) \qquad (1)$$

$\Delta \Phi_i$ = Decrease in angular intensity, at the i^{th} detector, from the value it would have for a nonabsorbing medium.

$\Psi(\vec{r})$ = Collision density at $\vec{r}$.

$P(\vec{r})$ = Contribution to the angular intensity at the i^{th} detector, due to one photon born at $\vec{r}$ per second.

$\Sigma_a(\vec{r})$ = Macroscopic absorption cross-section at $\vec{r}$.

$\Sigma_t(\vec{r})$ = Macroscopic total collision cross-section at $\vec{r}$.

Equation (1) may be discretized by dividing the medium up into a set of voxels, each sufficiently small that there is no significant variation of Ψ, P, or Σ_a/Σ_t within it. If these voxels are indexed by j, and each has volume V_j, the discrete version of (1) is

$$\Delta \Phi_i = \sum_j \frac{\Sigma_{aj}}{\Sigma_{tj}} \Psi_j P_{ij} V_j \qquad (2)$$

$$\equiv \sum_j \frac{\Sigma_{aj}}{\Sigma_{tj}} W_{ij} V_j \qquad (3)$$

The product $\Psi_j P_{ij}$ is the weight function, W_{ij}, for the i^{th} detector in the j^{th} voxel. Ψ_j is calculated directly by Monte Carlo as described above. The calculation of P_{ij} relies upon the reciprocity theorem [5],

$$G(\vec{r}, \hat{\Omega}; \vec{r}_o, \hat{\Omega}_o) = G(\vec{r}, -\hat{\Omega}; \vec{r}_o, -\hat{\Omega}_o) \qquad (4)$$

$G(\vec{r}, \hat{\Omega}; \vec{r}_o, \hat{\Omega}_o)$ is the angular intensity at $\vec{r}$ in direction Ω, per unit solid angle, due to one photon emitted per unit time at $\vec{r}_o$ in direction Ω_o.

Image Reconstruction: Use of a backprojection scheme to reconstruct images of subsurface absorbers was made possible by considering the distribution of photons which contribute to the detector response (i.e. the weight function), to be analogous to the straight line paths between source and detector in CT [6]. Assuming this analogy is appropriate, image reconstruction by backprojection becomes straightforward, though predictably it is computationally intensive. In the present scheme, the "measured attenuation", is projected back along those paths in the medium defined by the weight function. Attenuation is defined as the ratio of the intensity of backscattered light at a given position and orientation of a receiver from media with and without absorbers. Similar to the original CT algorithm, image reconstruction here is accomplished by the superposition of projected attenuation along paths defined by the weight function from multiple source-detector pairs.

Although a number of obvious problems present themselves with the above scheme (see below), for reasons not described here we felt the above scheme would be a reasonable starting point and should be rather robust.

RESULTS:

In an effort to relate the surface emission profile of backscattered photons to their 3-D distribution in the medium, we examined the histories of emerging photons to establish the relationship between various non-measurable parameters related to this distribution and the detector response. Parameters examined included the average number of collisions, **<n>**, the average total pathlength **<d>**, and the average maximum depth of penetration, **<Z>** of emerging photons. If it were to be found, as indeed it was, that these quantities had a systematic dependence on the medium's absorption cross-section and on the measurable properties of the intensity of the backscattered light and the geometry of the source-detector configuration, then we could conclude that selective interrogation is possible even for a medium that is homogeneous and scatters light isotropically. Some of these findings are shown in Figure 1, which shows in polar coordinates the dependence of the non-measurable quantities on the elevation and azimuthal angles of the detector.

In panel A the absorption cross-section is held constant at zero and the source-detector distance, ranging from 2 to 20 MFP in 2-MFP steps, is the parameter. **<Z>** is given by the distance from pole to curve. In panels B and C the source-detector distance is held constant at 5 MFP and the absorption cross-section, ranging from 0 to 10% of the total cross-section in 2% steps, is the parameter. **<Z>** is given by the distance from pole to curve in panel B, **<n>** by

the distance from pole to curve in panel C. A comparison of results shown in panels B and C demonstrate that the reduction in **<n>** per increment in absorption cross-section is greater than that observed for **<Z>** indicating that the ability to selectively probe the medium is enhanced with increasing background absorption.

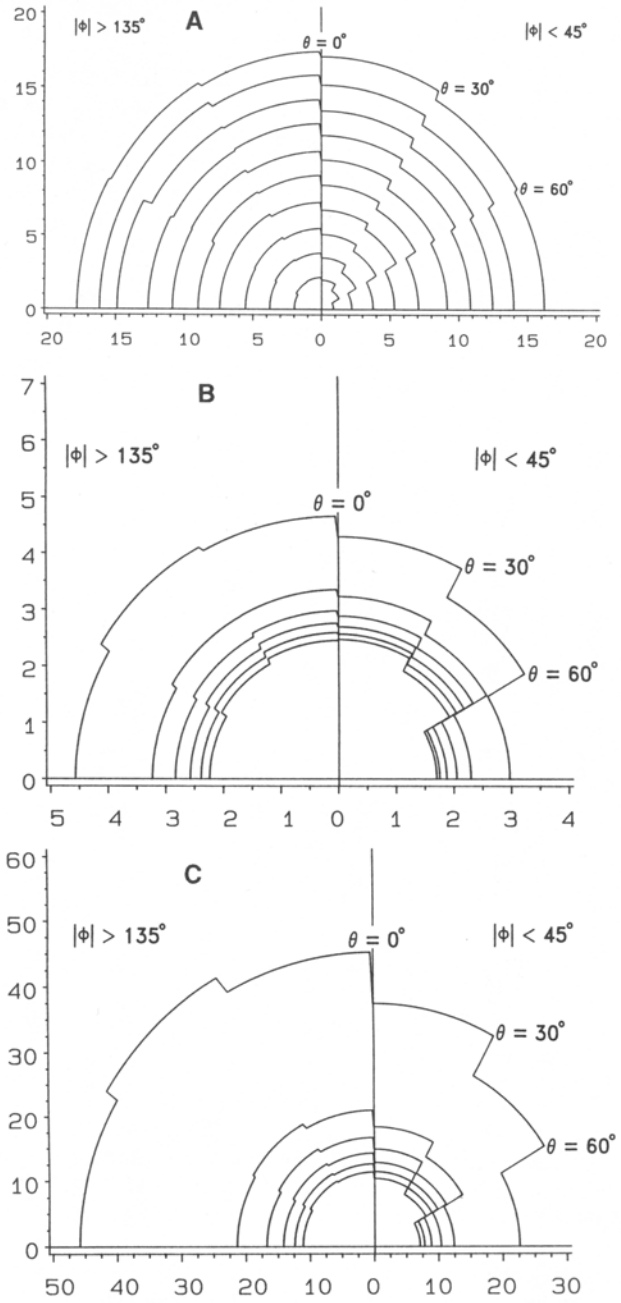

Figure 1. Dependence of **<Z>** and **<n>** on detector orientation. See text for description. Quantities of interest are proportional to the radial distances from pole to curve; numbers along the axes are in units of MFP (Panel A and B) and number of collisions (Panel C).

The above results demonstrated to us that even in the limit of isotropic scattering, selective interrogation of a random medium could be achieved by evaluating the surface emission profile of the backscattered light. Moreover, this ability was not diminished but, in fact, was enhanced by the presence of background absorption.

Having identified these relationships, we next turned our attention to relating the detected signal to the 3-D distribution of volume elements which contribute to the detector response. In the limit of weak absorption, this distribution can be exactly calculated by adopting the concept of importance sampling derived from transport theory [7]. As described in Methods the contribution of all points in space to the detector response is determined by the product of the flux and its adjoint at the point. In practice this is determined by the product of collision densities of photons launched from the source and the time reversal of photons entering the receiver. This product, when normalized, identifies the fractional contribution to the detector response of each volume element for a given source-detector configuration. Contour plots in the source-detector plane of these normalized weights are shown in Figure 2. In Figure 2A the source is located at (52,50,0) and the source and detector are both directed normally to the surface. In Figure 2B the source is at (55,50,0) and normally incident, while the detector direction is $\emptyset$ = 30°, Φ = 0°. In each region the accumulated weight is the indicated percentage of the total amount, proceeding from regions of greatest to least importance. Inspection reveals that, as expected, regions of greatest importance lie beneath the source and receiver and that this distribution is sensitive to the orientation of the receiver and its distance from the source.

Having examined the above, we then needed to explicitly make use of this information to reconstruct an actual 3-D image. To date we have considered several imaging schemes, although only a few have been directly tested. Shown here are results obtained using a modified backprojection scheme. The logic of this scheme was based on that originally employed for X-ray CT imaging and is described in Methods. Cross-sections of a calculated image using this algorithm are shown in Figure 3. Here the model medium contained an array of eight black cubes. Each of the absorbers measured 2 MFP on each edge and each was located at one of the corners of a 6x6x6 cubic-MFP volume whose shallowest boundary was 4 MFP below the surface of the surrounding medium. The medium itself was modeled to represent one which scattered light isotropically, was nonabsorbing and, except for the discrete absorbers, was homogeneous. At the depth modeled, the absorber array would not be discernible by eye if placed in a real medium having this composition. The image shown was obtained from the superposition of projected attenuations corresponding to over 92,000 weight functions.

Figure 3A shows a contour plot of the average intensity value of the image (1.0 being the darkest possible) in a 1-MFP-thick slab perpendicular to the medium's surface

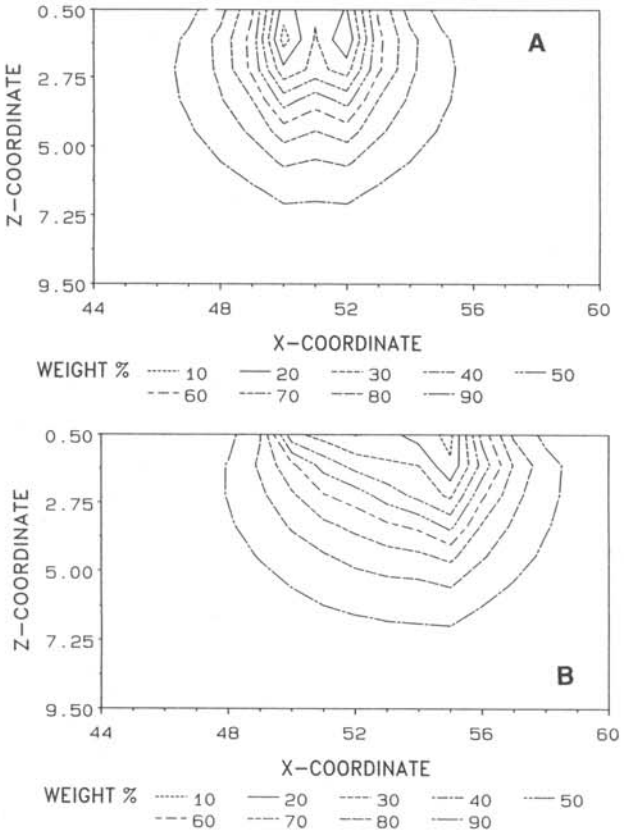

Figure 2. Contour plots of deciles of two weight functions; medium is 10 MFP thick with $\Sigma a/\Sigma t$ of 0.01. Plots shown were produced by ranking voxels in order of decreasing weight, and then converting from absolute units to percentages of the total weight of the medium.

(X-Z slice) bisecting the absorber array along one of the main axes. The dotted squares represent the actual spatial location of the absorbers. Inspection of the image reveals that the region of greatest darkening coincides almost precisely with the actual position of the absorbers. Figures 3B and 3C show views of the image from slices parallel to the surface and located 4-5 MFP and 11-12 MFP below the surface. In both cases clear evidence of the expected 4-fold symmetry is observed, and the regions of greatest darkening lie within the actual boundaries of the simulated absorbers.

DISCUSSION

The ability to generate even low resolution optical images of tissue based on NIR measurements could have enormous utility in clinical medicine. The known close relationship between oxidative metabolism and organ function indicates that such images could identify the physiological vitality of the tissues themselves. Based on the known pathlengths of light at these frequencies and our experience here, we estimate that the entire volume of a child and most of the volume of an adult would be accessible by an NIR-optical technique. The fact that an image can be calculated based on a backscatter measurement indicates that remote imaging may be possible.

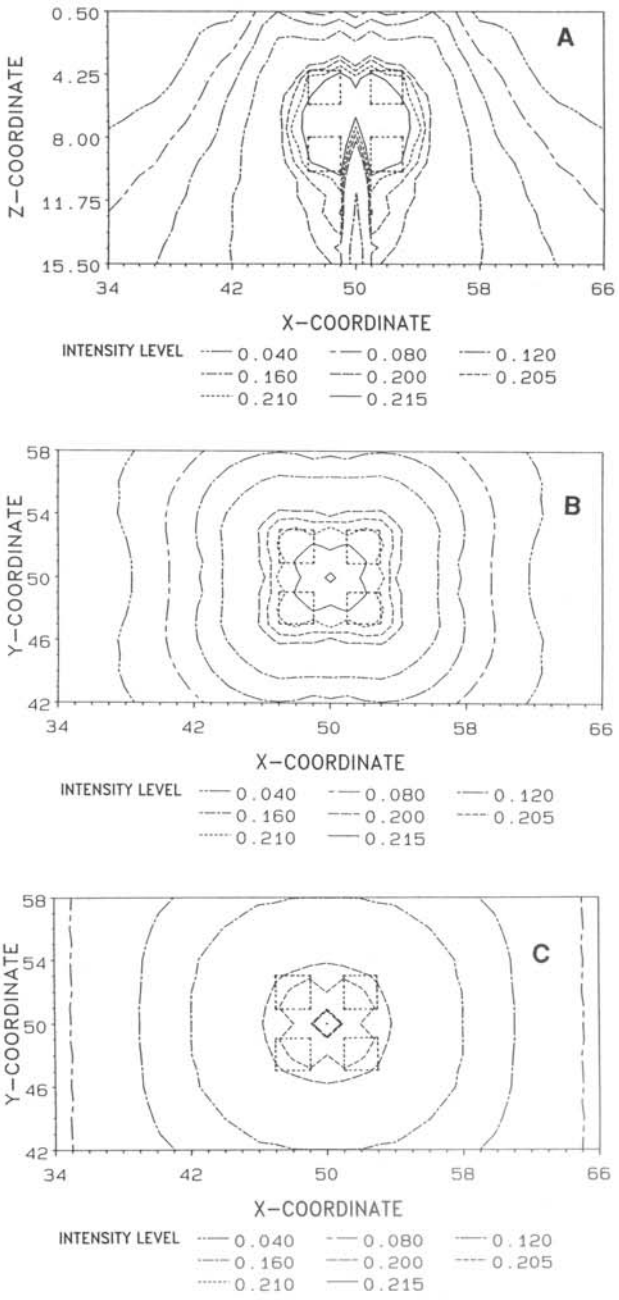

Figure 3. Image of cubical absorber array produced by unfiltered backprojection algorithm. See text for description.

Although it may be thought that results here will not generalize to complex real media (e.g. body tissue), in some respects the current model presents a more difficult problem. For example, light propagating through tissue is highly forward directed [8], permitting a tightly collimated beam to penetrate deeper than in the medium modeled here. In addition, unlike the present model, body tissues have numerous structures which could act as optical landmarks (e.g major vessels would appear as

strong local absorbers while tendons may behave as light guides) while having a known spatial location. While many obvious obstacles present themselves with the scheme described here for any practical system, we consider the demonstration that such images are even achievable significant.

FUTURE CONSIDERATIONS:

While images shown here are crude, improvements in image quality can reasonably be expected by including more source locations and by employing more tightly collimated receivers. The most important task before us at this point is to develop an analytical or iterative scheme for image deconvolution. Modification of the measurement scheme to include use of ultra-fast sources with a streak camera is also possible. The advantage of time-resolved techniques is that a smaller volume of medium will contribute to the detector response, thereby improving image resolution although at considerably higher equipment costs. Other measurement schemes could include detection of Doppler shifts together with the backscatter intensity measurements. By backprojecting Doppler shifts along paths defined by the weight functions, optical images of flow could be achieved.

REFERENCES

[1] F.F. Jobsis, "Noninvasive, infrared monitoring of cerebral and myocardial oxygen sufficiency and circulatory parameters", J. Appl. Physiol. 43, 858-872, 1977.

[2] R. Aronson, R.L. Barbour, J. Lubowsky, and H. Graber, "Application of transport theory to NIR medical imaging", in Modern Mathematical Models in Transport Theory, Berkhauser Press, 1990, in press.

[3] R.L. Barbour, H. Graber, J. Lubowsky, and R. Aronson, "Monte Carlo (MC) modeling of photon transport in tissue", Abst. 599-603, Biophys. J. 57, 381a-382a, 1990.

[4] M.H. Kalos, and P.A. Whitlock, Monte Carlo Methods, Vol 1, John Wiley and Sons, New York,1986.

[5] K.M. Cose and P.F. Zweifel, Linear Transport Theory, Addison-Wesley Publishing Co., Reading, MA, 1967.

[6] R.A. Brooks, and DiChiro, G., "Principles of computer assisted tomography (CAT) in radiographic and radioisotopic imaging", Phys. Med. Biol., 21, 689-732 (1976).

[7] J.R. Lamarsh, Nuclear Reactor Theory, Addison-Wesley Publishing Co., Reading, MA, 1966.

[8] B.C. Wilson, W.P. Jeeves, and D.M. Lowe, In vivo and post mortem measurements of the attenuation spectra of light in mammalian tissues, Photochem. Photobiol., 42, 153-162, 1985.